Available online at www.sciencedirect.com
ScienceDirect
Journal of Nuclear Materials 367–370 (2007) 829–833
journal of nuclear materials
www.elsevier.com/locate/jnucmat

Features of dislocation channeling in neutron-irradiated V–(Fe, Cr)–Ti alloy

Ken-ichi Fukumoto [a,*], Masanari Sugiyama [b], Hideki Matsui [b]

[a] Graduate School of Nuclear Power and Energy Safety Engineering, University of Fukui, Fukui 910-8507, Japan
[b] IMR/Tohoku University, 2-1-1 Katahira, Aoba-ku, Sendai 980-8577, Japan

Abstract

Post-irradiation annealing experiments were used to study the recovery of microstructure and mechanical properties in V–Cr–Ti and V–Fe–Ti alloys irradiated at 228 °C to 4 dpa. After 500 °C post irradiation annealing, dislocation channeling occurred at deformed area in tensile specimens and significant loss of ductility resulted. For post irradiation annealing above 600 °C, recovery of damage structure and tensile properties occurred and irradiation hardening completely disappeared in V–3Fe–4Ti–0.1Si. Clear dislocation channels can be seen mainly in deformed areas of specimens showing significant loss of ductility, however, a pile-up of dislocations in channels was observed at a grain boundary where the channel did not penetrate into the adjacent grain. It is assumed that defect clusters were absorbed by mobile dislocations and no debris or segments of defect clusters were left in clear channels of bcc metals and alloys under post-irradiation deformation.

1. Introduction

Vanadium-based alloys have been developed as candidate materials for structures of fusion power reactors because of their potential for low activation and attractive high-temperature properties [1]. However, some studies have reported that significant radiation hardening and embrittlement occurred in V–4Cr–4Ti irradiated by neutrons at 100–400 °C to a few displacement per atom (dpa) [2,3]. This degradation of properties may be attributed to a high density of fine defect clusters and their response to deformation. Dislocation channels have been observed in deformed V–4Cr–4Ti alloys irradiated with neutrons below 300 °C [4]. The local deformation due to the formation of dislocation channels gives rise to plastic instability and leads to significant loss of ductility. In order to understand the thermal stability of defect clusters and radiation anneal hardening, post-irradiation annealing experiments have been utilized to evaluate the recovery of microstructure and mechanical properties in vanadium alloys irradiated below 300 °C [5,6]. However, there are few data for post-irradiation annealing and radiation anneal hardening in V–Ti alloys including V–Cr–Ti alloys.

In this study, experiments to determine the post-irradiation annealing effect on mechanical properties and microstructures in neutron-irradiated V–Cr–Ti and V–Fe–Ti alloys are described.

* Corresponding author. Tel./fax: +81 776 27 9712.
E-mail address: fukumoto@mech.fukui-u.ac.jp (K.-i. Fukumoto).

0022-3115/$ - see front matter © 2007 Elsevier B.V. All rights reserved.
doi:10.1016/j.jnucmat.2007.03.075

Neutron-irradiated and post-irradiation annealed specimens were tensile tests at room temperature. Microstructural observation of as-irradiated and post-irradiation annealed specimens revealed the interior structure of dislocation channels and the microstructural evolution of the damage structure during post-irradiation annealing.

2. Experimental procedures

The majority of test specimens for this study were prepared from V–4Cr–4Ti and V–3Fe–4Ti–Si alloys. The specimens are described in detail in Ref. [7]. The mean size of grains was about 26 μm and 30 μm for V–4Cr–4Ti and V–3Fe–4Ti–Si alloys, respectively. The tensile specimens for this study were of type SSJ and had nominal gauge dimensions of 0.25 mm $(t) \times 1.2$ mm $(w) \times 5$ mm (l). Tensile specimens and TEM specimens were punched from cold-rolled sheets with the longitudinal direction parallel to the rolling direction. Before irradiation, all specimens were annealed in vacuum at 1000 °C for 2 h.

The specimens were irradiated in the A1 position in ATR [8]. As ATR is water-cooled mixed spectrum reactor, a thermal neutron filter of gadolinium was incorporated to minimize the V-to-Cr transmutation. In the ATR-A1 irradiation, high-purity lithium was used to bond the specimens to the sub-capsules for impurity control and temperature uniformity. The experiment achieved a peak neutron damage of 4.7 dpa. Nominal irradiation temperature was 228 °C. Post-irradiation annealing was carried out for 2 h at temperatures, 500 °C, 600 °C and 700 °C in a vacuum better than 5×10^{-4} Pa at the Oarai branch, IMR/Tohoku Univ. Tensile tests were conducted at room temperature and strain rates of 0.2 mm/min and 0.02 mm/min, i.e. 6.67×10^{-4}/s and 6.67×10^{-5}/s. Some specimens of V–4Cr–4Ti alloys were used to determine the strain rate sensitivity of yield stress and UTS with strain rates from 6.67×10^{-6}–6.67×10^{-2}/s. TEM samples were punched from non-deformed areas of tested specimens. The microstructural observations used a JEM-2000 FX operating at 200 kV.

3. Results

Stress–strain curves of irradiated and annealed V–4Cr–4Ti alloys are plotted in Fig. 1. Significant loss of ductility and irradiation hardening can be seen in the as-irradiated V–4Cr–4Ti alloy. Following yielding, the irradiated specimens failed rapidly owing to plastic instability. A strain rate sensitivity of V–4Cr–4Ti irradiated at 228 °C was obtained and the value m of strain rate sensitivity for yield stress was 0.022 for the strain rate range 6.67×10^{-6}–6.67×10^{-2}/s at room temperature. The strain rate sensitivity at room temperature for V–4Cr–4Ti alloy did not differ so much before (0.018) and after neutron irradiation [9]. In a specimen annealed at 500 °C, the yield stress and ultimate tensile stress (UTS) were slightly lower than the as-irradiated specimens but the loss of ductility was not recovered and uniform elongation was less than 1%. As annealing temperature was increased, the irradiation hardening decreased and the ductility recovered. Fig. 2 shows changes of the yield stress,

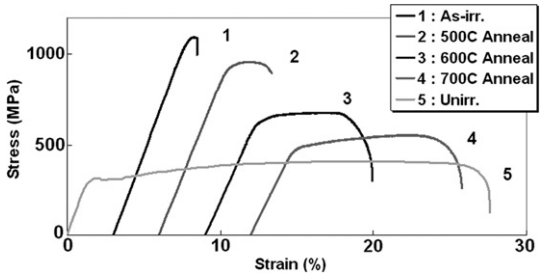

Fig. 1. Stress–strain curves at room temperature for neutron irradiated V–4Cr–4Ti alloys after post-irradiation annealing.

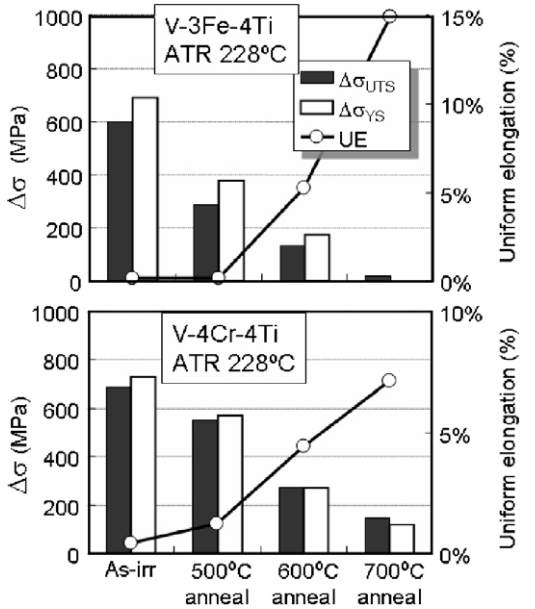

Fig. 2. Changes of room temperature yield stress, UTS and uniform elongation in V–4Cr–4Ti and V–3Fe–4Ti–0.1Si alloys for different post-irradiation annealing temperatures.

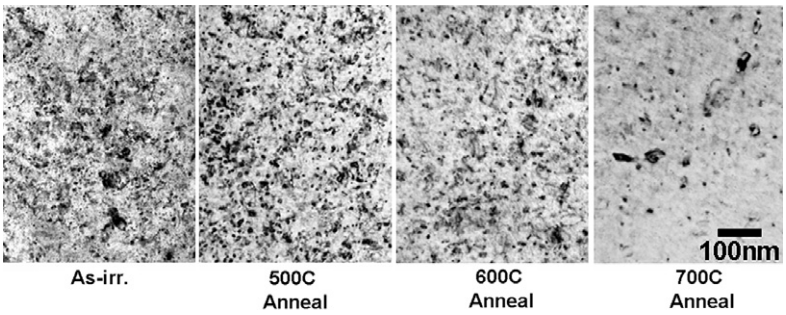

Fig. 3. Microstructures of neutron-irradiated V–4Cr–4Ti alloys after post-irradiation annealing.

UTS and the uniform elongation in V–4Cr–4Ti and V–3Fe–4Ti–0.1Si alloys due to post-irradiation annealing at different temperatures. When the annealing temperature was above 600 °C, the recovery of mechanical properties appeared significantly in both V–Cr–Ti and V–Fe–Ti alloys. For 700 °C annealing, the irradiation hardening in V–3Fe–4Ti–0.1Si completely disappeared and the uniform elongation recovered to the level of unirradiated specimens, 15%.

The changes in damage microstructure of V–4Cr–4Ti for different post-irradiation annealing temperatures are shown in Fig. 3. The density of defect clusters was very high and their size was very small, about a few nm, in the as-irradiated specimens. After 500 °C annealing, the density of defect clusters was almost the same as in as-irradiated specimens. With increasing annealing temperature above 600 °C, the defect clusters were removed. The clusters grew into large dislocation loops on annealing at 600 °C. The large loops in V–3Fe–4Ti–0.1Si were identified as lying on the (1 1 1) plane with $a/2\langle 1\,1\,1\rangle$ Burgers vector. No Ti(OCN) precipitates could be seen in the as-irradiated and annealed V–Cr–Ti and V–Fe–Ti alloys. Changes with annealing temperatures of the density and average size of defect clusters or dislocation loops in V–3Fe–4Ti–0.1Si alloys are shown in Fig. 4, and the relevant size distribution of loops and defect clusters are given in Fig. 5 as a function of annealing temperature. The density of defect clusters in V–4Cr–4Ti could not be measured because no flat surface area was obtained in electro-polished TEM specimens. It can be noted that the density of small loops is less in the V–3Fe–4Ti–0.1Si annealed at 600 °C than in the as-irradiated state or annealed at 500 °C. Furthermore, larger defect clusters or dislocation loops annealed out in the V–3Fe–4Ti–0.1Si at 700 °C, while the density of tangled dislocation increased. An estimation of yield stress increase based on the measured defect structure parameters in the irradiated and annealed V–3Fe–4Ti–0.1Si was reported in [10]. The estimation of irradiation hardening by microstructural analysis showed the result approximately similar to experimental results,

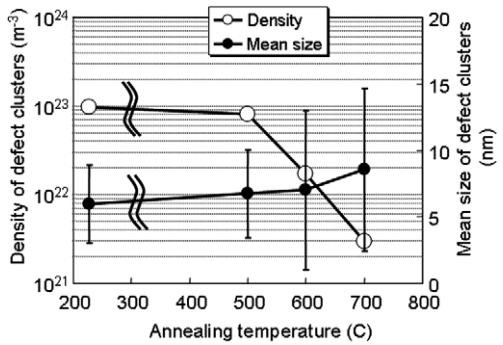

Fig. 4. Post-irradiation annealing temperature dependence of density and mean size of defect clusters in the V–3Fe–4Ti–0.1Si alloy irradiated at 228 °C.

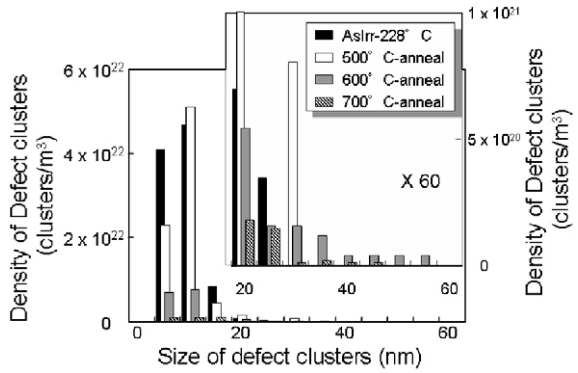

Fig. 5. Size distribution of defect clusters in the V–3Fe–4Ti–0.1Si alloy irradiated at 228 °C after post-irradiation annealing. Note the difference of scale of vertical axis for density of dislocation loops in the right figure.

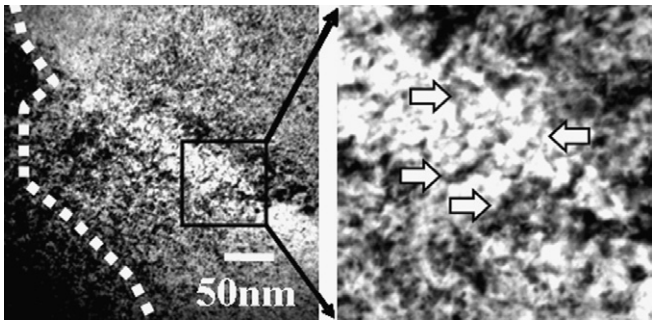

Fig. 6. Examples of dark field images of a dislocation channel close to a grain boundary where the dislocation channels could not penetrate across the boundary. The right micrograph magnified the image of the interior of a dislocation channel. A broken line in the left figure shows the grain boundary and arrows in the right figure indicate the tangled dislocations in channel.

except for the estimation of the hardening about 50 MPa at 700 °C due to the residue of dislocation loops in spite of no irradiation hardening in experimental results at 700 °C.

TEM observation in deformed areas close to the fracture was also performed and compared to undeformed area. It should be noted that no dislocation channels were observed in the specimens annealed above 600 °C for either V–4Cr–4Ti or V–3Fe–4Ti–0.1Si. Fig. 6 shows the dark field images of a dislocation channel in V–3Fe–4Ti–0.1Si annealed at 500 °C. The images were taken from a thin area close to a grain boundary where the dislocation channel did not penetrate into the neighboring grain and a large strain field extended around the grain boundary. Several dislocation lines could be seen inside the channel and were likely the result of a pile up close to the grain boundary (see the right photo in Fig. 6).

4. Discussion

In vanadium and vanadium alloys, radiation anneal hardening has been reported for specimens irradiated at low temperature, below 200 °C [5,6,11]. Radiation anneal hardening was observed on annealing between room temperature and 200 °C and most of the recovery, back to the unirradiated yield stress, occurred at 400–600 °C [6]. The main feature of recovery behavior in this study is in good agreement with the previous results. However, the recovery of damage structure and irradiation hardening in V–3Fe–4Ti–0.1Si alloys for annealing above 600 °C, especially at 700 °C was more pronounced than in any other vanadium alloys. The rapid recovery in V–Fe–Ti alloy for post-irradiation annealing experiments may be explained by the effect of atomic size factor of undersized solute atoms. From irradiation creep tests and thermal creep tests of V–3Fe–4Ti–0.1Si alloy, the thermal creep strain rate was faster than in V–4Cr–4Ti [8] and the effective strain from irradiation creep was larger than in V–4Cr–4Ti for the same irradiation condition [12]. It is concluded that the vacancy diffusion during thermal creep and irradiation creep is assisted by the addition of undersized solute iron atoms that are smaller than chromium atoms in vanadium alloys. The vacancy diffusion mechanism in V–Fe–Ti alloys may also be related to the appearance of the giant swelling as a result of the enhancement of vacancy diffusion [13].

Most channels were clear dislocation channels showing no dislocation walls or dislocation forest at the interface between channel and matrix or inside the channels. These same dislocation channel features have been reported in many fcc metals and alloy for example, [14]. From molecular dynamic computer simulation study in bcc-iron by Nomoto [15], the SIA loops with $\langle 1\,1\,1\rangle$ type of Burgers vector are absorbed by edge dislocations to form a large super-jog during interaction between the SIA loop and the edge dislocation. The interaction mechanism can be explained athermally by the elastic interactions between dislocation segments. No debris or segments of SIA loops are left after the edge dislocation passed over the SIA loop, even though the directions of Burgers vectors of SIA loop and edge dislocation are different. This result suggests that formation of dislocation channeling in bcc-iron and vanadium alloys is feasible when matrix damage is primarily SIA loops. Clear channels can be formed in bcc metals and alloys without hard inclusion like hard precipitates in matrix. The

defect clusters formed below 300 °C are soft obstacle for dislocation movement at stress level above 700 MPa and are dissolved by the interaction with mobile dislocations. However, hard inclusion like high-angle random-oriented grain boundaries stops the propagation of clear channels at the grain boundary because the dislocations cannot transfer through the misoriented lattice configuration of a random grain boundary. The stress concentration factor at the front of a dislocation pile-up can be large; if there are only 10 dislocations in the pile-up then the stress concentration factor may be as large as 3. The pile-up microstructure in otherwise clear channels, therefore, could only be seen near grain boundary. This grain boundary configuration is one of the rate-controlling factors for the propagation of dislocation channels. It affects the flow localization for increasing stress concentration and leads to the necking deformation in localized area and significant loss of ductility.

5. Conclusion

Post-irradiation annealing experiments were used to study the recovery of microstructure and mechanical properties in V–4Cr–4Ti and V–3Fe–4Ti–0.1Si alloys irradiated at 228 °C to 4 dpa in ATR.

The recovery of damage structure and tensile properties occurred in post-irradiation anneal treatment above 600 °C. Irradiation hardening completely disappeared in V–3Fe–4Ti–0.1Si after anneal at 700 °C.

Clear dislocation channels can be seen mainly in deformed areas of specimens showing significant loss of ductility, however, a pile-up of dislocations in channels was observed at a grain boundary where the channel did not penetrate into the adjacent grain. It is assumed that defect clusters were absorbed by mobile dislocations and no debris or segments of defect clusters were left in clear channels in vanadium alloys. The grain boundary configuration is one of the important factors for the formation and propagation of dislocation channels during deformation.

Acknowledgement

This work is partly supported by National Institute for Fusion Science for installing a vacuum furnace in radiation controlled area in the Oarai branch of IMR/Tohoku Univ.

References

[1] H. Matsui, K. Fukumoto, D.L. Smith, Hee M. Chung, W. van Witzenburg, S.N. Votinov, J. Nucl. Mater. 233–237 (1996) 92.
[2] S.J. Zinkle, H. Matsui, D.L. Smith, A.F. Rowcliffe, E. van Osch, K. Abe, V.A. Kazakov, J. Nucl. Mater. 258–263 (1998) 205.
[3] P.M. Rice, S.J. Zinkle, J. Nucl. Mater. 258–263 (1998) 1414.
[4] M. Sugiyama, K. Fukumoto, H. Matsui, J. Nucl. Mater. 329–333 (2004) 411.
[5] K. Shiraishi, K. Fukaya, Y. Katano, J. Nucl. Mater. 54 (1974) 275.
[6] M.S. Wechsler, K.L. Murty, Metal. Trans. A 20A (1989) 2637.
[7] K. Fukumoto, T. Morimura, T. Tanaka, A. Kimura, K. Abe, H. Takahashi, H. Matsui, J. Nucl. Mater. 239 (1996) 170.
[8] K.-i. Fukumoto, H. Matsui, H. Tsai, D.L. Smith, J. Nucl. Mater. 283–287 (2000) 492.
[9] M. Koyama, K. Fukumoto, H. Matsui, J. Nucl. Mater. 329–333 (2004) 442.
[10] K.-i. Fukumoto, H. Matsui, Y. Candra, K. Takahashi, H. Sasanuma, S. Nagata, K. Takahiro, J. Nucl. Mater. 283–287 (2000) 492.
[11] Y. Huang, R.J. Arsenault, Rad. Effects 17 (1973) 3.
[12] K. Fukumoto, S. Takahashi, R.J. Kurtz, D.L. Smith, H. Matsui, J. Nucl. Mater. 341 (2005) 83.
[13] K. Fukumoto, A. Kimura, H. Matsui, J. Nucl. Mater. 258–263 (1998) 431.
[14] D.J. Edwards, B.N. Singh, J.B. Blide-sorensen, J. Nucl. Mater. 342 (2005) 164.
[15] A. Nomoto, N. Soneda, A. Takahasi, S. Ishino, Mater. Trans. 46 (2005) 463.